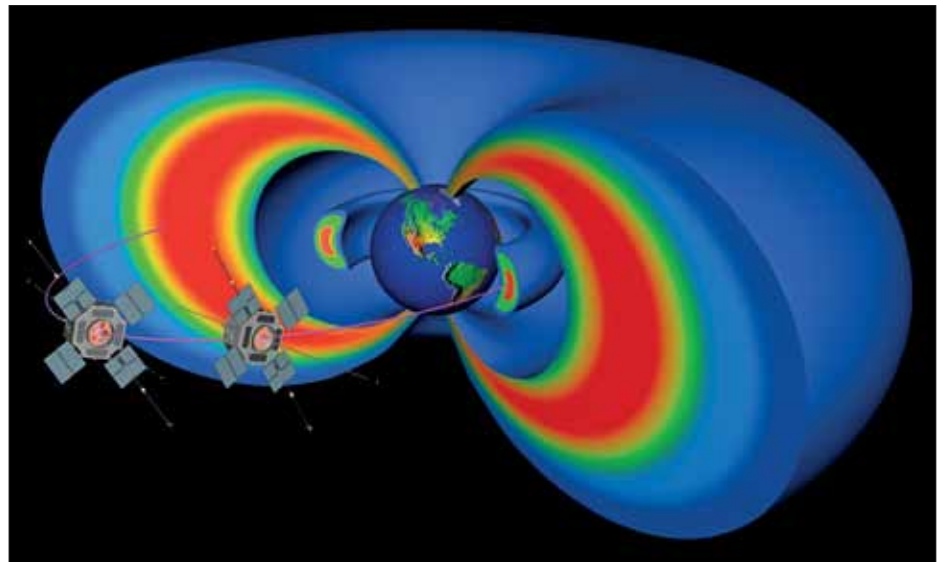# Solving the radiation belt riddle

DP Hartley and MH Denton present a guide to phase space density, setting out how this measure is calculated and how it is used to identify source and loss processes in the radiation belts.

The radiation belts – areas around the Earth where high-energy charged particles are trapped by the planet's magnetic field – are complex regions influenced by factors such as the solar wind, particle interactions and solar activity. Understanding them is important because of the potential damage that high-energy particles can inflict. The ability to interpret satellite measurements of electron flux at a single position and time – in parallel with the variations of the geomagnetic field – is essential to advance the understanding of radiation belt dynamics. Phase space density (PSD) is a calculated quantity that can account for these magnetic fluctuations because it exists in a coordinate system relating to the trajectories of radiation belt particles. We provide a step-by-step review of the techniques used to convert measured electron fluxes to phase space density, independent of satellite instrumentation and detailed analysis. In addition, we discuss examples of how specific source and loss processes might be observed in the phase space density signature. We hope that this review of PSD calculation techniques will prove useful for newcomers to this exciting and burgeoning field.

Radioactivity

In 1958, the Explorer I spacecraft launched, carrying an experiment designed by James Van Allen (Van Allen *et al.* 1959, Van Allen and Frank 1959). Intended to measure cosmic rays, the instrumentation was also sensitive to highly energetic electrons. Measurements revealed energetic electrons encompassing the Earth – something that led Van Allen's colleague Ernie Ray to state, famously: "Space is radioactive!" This inadvertent discovery prompted research into what are now known as the Van Allen radiation belts – two toroidal regions of energetic particles constrained within the Earth's magnetic field (see figure 1).

The processes that fuel the belts' high degree

1: A representation of the Van Allen radiation belts with two spacecraft, representing the Van Allen Probes, and their orbit through the heart of the radiation belts. (JHU/APL, NASA)

of variability are of great interest to the scientific community. While many source and loss processes have been identified (e.g. Friedel *et al.* 2002, Liemohn and Chan 2007), quantitative understanding of how these processes wax and wane between different events remains elusive. Interactions with various electromagnetic waves can pitch-angle scatter electrons and thus enhance losses to the atmosphere. In contrast, radial diffusion processes can transport electrons outwards, leading to losses to the magnetopause. With observational evidence available in support of both processes, it is the quantification of the relative contribution from each mechanism that needs to be addressed. It has become clear that a complete and accurate predictive capability will be hard to achieve until these mechanisms are better understood. Energetic electron flux in the outer radiation belt can vary by up to five orders of magnitude in only a few hours (e.g. Baker *et al.* 2007, Horne *et al.* 2009), meaning that a high degree of spatial and temporal resolution is required in order for the mysteries behind these processes to be unravelled.

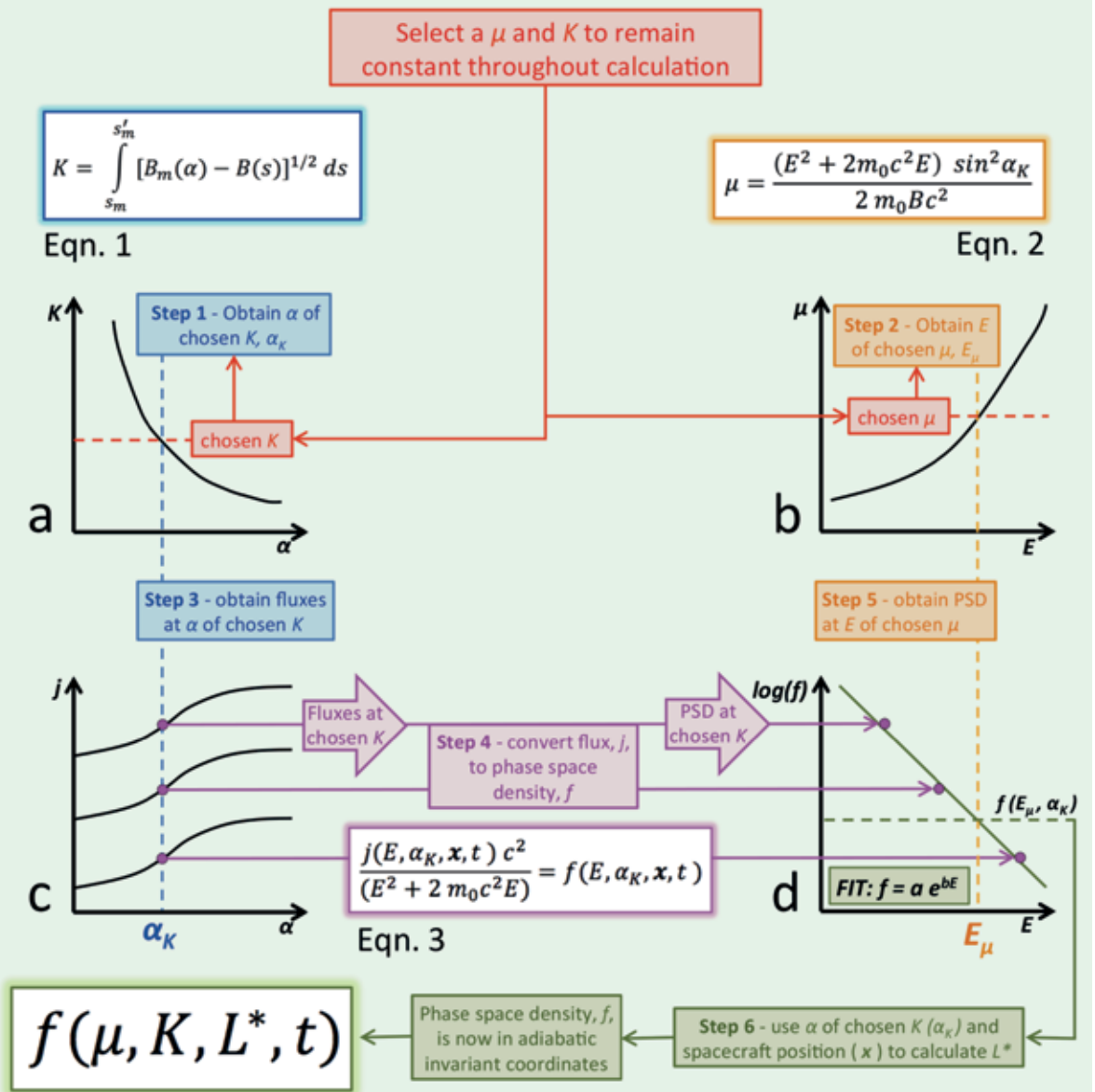In 2012, more than 50 years since the discovery of the radiation belts, the high-profile NASA Van Allen Probes mission was launched successfully. Onboard the two identical spacecraft are detectors designed specifically to study the particles of the radiation belts in high temporal and spatial resolution. With interest in radiation belt dynamics heightening during the Van Allen Probes mission, there has been a rapid output of new and exciting research results that implement the PSD calculation. This article is intended to supplement these publications by providing a thorough description of the PSD calculation that is independent of detailed analysis of any individual event.

Particle detectors typically measure the electron flux at a distinct set of parameters: energy E, pitch angle α, position x, and time t. In turn, each of these parameters relates to one or more of the adiabatic invariants associated with electron motion in the geomagnetic field. The first adiabatic invariant, μ (associated with the gyro-motion of a particle about a magnetic field line), is dependent upon both the particle's pitch angle (the angle between the particle's velocity vector and the magnetic field vector) and the particle's energy. The second adiabatic invariant, K (related to

> **"The Van Allen Probes mission has prompted exciting results using the phase space density calculation"**

2: A schematic representation of the phase space density calculation. Initially, a value of μ and K are selected to remain constant throughout the calculation. Panel (a) shows schematically the relationship between the second adiabatic invariant, K, and pitch angle, α, for one instance of time, calculated using equation 1. The dashed red line indicates the selected value of K, and the dashed blue line indicates the pitch angle that corresponds to the selected K, α_K. (b) is a representation of the relationship between μ and E (calculated using equation 2), for the pitch angle obtained in (a), α_K. The dashed red line indicates the selected value of μ and the dashed orange line indicates the energy that corresponds to the selected value of μ, E_μ. (c) represents the electron flux pitch-angle distribution for three instrument energy channels. The

Select a μ and K to remain constant throughout calculation

$$K = \int_{s_m}^{s_m'} [B_m(\alpha) - B(s)]^{1/2}\, ds$$

Eqn. 1

$$\mu = \frac{(E^2 + 2m_0c^2E)\ \sin^2\alpha_K}{2\, m_0 B c^2}$$

Eqn. 2

Step 1 - Obtain α of chosen K, α_K

chosen K

Step 2 - Obtain E of chosen μ, E_μ

chosen μ

Step 3 - obtain fluxes at α of chosen K

Step 5 - obtain PSD at E of chosen μ

Fluxes at chosen K

Step 4 - convert flux, j, to phase space density, f

PSD at chosen K

$$\frac{j(E,\alpha_K,x,t)\,c^2}{(E^2 + 2\,m_0c^2E)} = f(E,\alpha_K,x,t)$$

Eqn. 3

$f(E_\mu, \alpha_K)$

FIT: $f = a\,e^{bE}$

E_μ

$$f(\mu, K, L^*, t)$$

Phase space density, f, is now in adiabatic invariant coordinates

Step 6 - use α of chosen K (α_K) and spacecraft position (x) to calculate L^*

dashed blue line indicates the pitch angle that corresponds to the selected K, α_K, from (a). From these pitch-angle distributions, it is possible to read the electron flux values at the pitch angle α_K to obtain a set of flux values that vary with instrument energy channels. These flux values are then converted to PSD using equation 3 (where E is the central energy of the satellite instrument channel).
Panel (d) displays these PSD values, calculated using the fluxes from (c), as a function of the instrument energy channels. Fitting a function to these values of the form shown in (d) and using the energy corresponding to the selected value of μ, E_μ, from panel (b), it is possible to obtain the PSD corresponding to selected values of μ and K, $f(E_\mu, \alpha_K)$. Using α_K and the spacecraft position x, the IRBEM library is used to calculate L^*. The electron PSD has now been calculated in adiabatic invariant coordinates for one instance of time. This process can be repeated for the required number of time intervals.

a particle's bounce motion along a magnetic field line between the magnetic mirror points), depends upon pitch angle, while the inverse of the third adiabatic invariant, L^* (related to a particle's drift motion about the Earth), depends upon both position and pitch angle. A full definition of the adiabatic invariants is given by Schulz and Lanzerotti (1974), Walt (1994) and Green and Kivelson (2004). The aim of this article is to provide a step-by-step review of the techniques used to convert measured electron fluxes to phase space density (PSD), independent from satellite instrumentation and detailed analysis. In order to follow the steps outlined

in this article, electron flux measurements are required to be resolved in terms of both pitch-angle and energy.

PSD is used in multiple fields of physics research such as quantum mechanics, thermodynamics, astrophysics and space science. Here, we discuss how PSD can assist in differentiating between source mechanisms, as well as being used to identify loss processes, for radiation belt dynamics.

In the context of the radiation belts, PSD is defined as the electron flux divided by the square of the momentum (e.g. Chen *et al.* 2007). It is therefore possible to convert measured electron

fluxes to PSD and obtain the corresponding adiabatic invariants. This, however, would result in PSD values with different adiabatic invariants at each instant of time. Typically, values for the first and second adiabatic invariants are selected to remain constant for the duration of a study, thus allowing determination of the variations in PSD and L^*. Converting to PSD, which uses a coordinate system aligned with radiation belt particle trajectories, allows the geomagnetic field variations to be considered in parallel with electron flux variations. This technique has been developed and described in detail in several studies using electron flux meas-

3: Schematic diagram showing how internal and external acceleration may appear in the PSD vs $L*$ profile (adapted from Green and Kivelson 2004). Panel (a) shows a PSD increase caused by radial diffusion from an external source mechanism, whereas panel (b) indicates a PSD increase caused by a local internal acceleration mechanism. The red lines indicate the PSD vs $L*$ profile prior to acceleration (time = t_1) with the blue line showing the effect of the acceleration event (time = t_2).
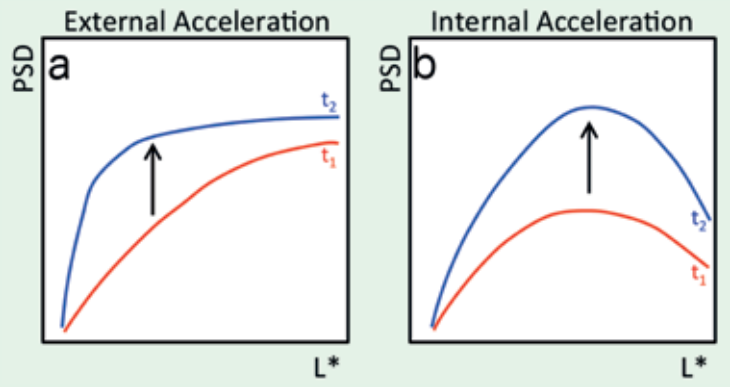
urements from different spacecraft (e.g. Hilmer *et al.* 2000, Green and Kivelson 2004, Chen *et al.* 2006, Shprits *et al.* 2012). Descriptions of how signatures of different physical mechanisms might be observed in the PSD vs $L*$ profile have also been produced (e.g. Turner *et al.* 2012, Reeves *et al.* 2013).

Methodology

Because *in situ* observations of the geomagnetic field provide measurements at only one location on a magnetic field line, it is necessary to implement a magnetic field model in order to calculate the second adiabatic invariant, K, and the inverse of the third invariant, $L*$. If using measurements from a spacecraft without a magnetometer onboard, it is necessary to use a magnetic field model for the calculation of all three adiabatic invariants. Calculating the PSD at chosen values of μ and K can be performed in six steps:

1. Calculate the pitch angle of chosen K
2. Calculate the energy of chosen μ and K
3. Calculate the fluxes (for each energy channel) at chosen K
4. Convert these fluxes at chosen K to PSD
5. Calculate the PSD at chosen μ and K
6. Calculate $L*$.

Once these steps have been carried out (as summarized in figure 2), the PSD vs $L*$ profile can be interpreted to provide evidence for active source and loss processes. For step 1, to calculate the second adiabatic invariant, K, as a function of pitch angle and time, it is common to use the International Radiation Belt Environment Modeling Library (IRBEM-LIB [2004-2012]) and equation 1. This relationship is shown schematically in figure 2a.

$$K = \int_{s_m}^{s'_m} [\mathbf{B}_m(\alpha) - \mathbf{B}(s)]^{1/2} \, ds \qquad (1)$$

The IRBEM-LIB is a set of source code dedicated to modelling the radiation belts and is available at http://sourceforge.net/projects/irbem/files. Depending upon the chosen magnetic field model, the IRBEM library requires different solar wind parameters and geomagnetic activity indices as drivers (e.g. disturbance-storm-time index, solar wind dynamic pressure,

interplanetary magnetic field, etc). These can be obtained from OMNIweb (King and Papitashvilli 2005), a database of solar wind observations propagated to the Earth's bowshock. Various functions within the IRBEM-LIB can be used, with some directly providing adiabatic invariants or related quantities as outputs. IRBEM-LIB is used to obtain a value for quantity, I, in small increments of pitch angle, at each instance of time. This value, I, is related to the second adiabatic invariant, K, through the equation; $K = I\sqrt{\mathbf{B}_m}$ where $\mathbf{B}_m$ is the magnetic field at the mirror point, which can also be output by the library functions. It is then possible to interpolate between the calculated $K(\alpha)$ values to obtain a pitch angle for any desired K at each instance of time (figure 2a). (Common units for the second adiabatic invariant, K, are $G^{1/2}$km; model output units are: I in Earth radii, R_E, and $\mathbf{B}_m$ in nT, yielding units of $nT^{1/2}R_E$.) A value of the second invariant, K, is selected to remain constant throughout the calculations. This, in turn, yields a pitch angle of fixed K, which will be referred to as α_K hereafter (see figure 2a). While K is kept constant over time, the pitch angle at fixed K temporally evolves due to the varying input solar wind conditions that drive the magnetic field model. The pitch angle obtained, α_K, is also used in calculation of the first and third adiabatic invariants.

Step 2 involves calculating the energy of chosen μ and K (figure 2b) by using equation 2. This relationship is shown schematically in figure 2b.

$$\mu = \frac{(E^2 + 2m_0c^2E)\sin^2\alpha_K}{2m_0\mathbf{B}c^2} \qquad (2)$$

If using measurements from a spacecraft with a magnetometer onboard, the measured magnetic field can be used in the calculation of μ, otherwise it is required to implement the model magnetic field. Because μ is pitch-angle dependent, the pitch-angle of chosen K, α_K, is used. Calculating μ over small intervals of energy negates the complication of solving equation 2 for E. It is thus possible to interpolate between these calculated μ values, obtaining the energy corresponding to the chosen value of μ, E_μ, at a single instance of time (see figure 2b). Typical units for μ are MeV/G and care must be taken to

avoid confusion between units of energy (m_0c^2 is in Joules, whereas units for E are likely to be in eV, keV or MeV).

Step 3, calculating the flux (for each energy channel) at chosen K, requires performing a fit of the pitch angles to the measured electron flux, j (see figure 2c). This is required at each of the instrument energy channels available. There are several methods available for calculating the full pitch angle distributions, such as fitting sums of powers of trigonometric functions (e.g. Green and Kivelson 2004) or to invert an accurate pitch-angle distribution using optimal estimation (e.g. Selesnick and Blake 2000, Hartley *et al.* 2013). After obtaining the full pitch-angle distribution, it is possible to determine the flux at pitch angle, α_K, for each energy channel. This, in turn, yields a set of flux values at constant K, varying in energy.

In step 4, using equation 3, the flux values obtained for the selected value of K are converted to PSD.

$$\frac{j(\mu,K,\boldsymbol{x},t) \times c^2}{(E^2 + 2m_0c^2E)} = f(\mu,K,\boldsymbol{x},t) \qquad (3)$$

The energies, E, to be used in this equation are the central energies of the satellite instrument channels. Again, the user needs to be aware of different units of energy. These calculated PSD values are at the chosen value of K, varying in energy.

Through step 5 it is now possible to produce a fit of these PSD values of chosen K against energy using an equation of the form, $f = ae^{bE}$ where f is PSD, E is energy and a and b are the fit coefficients. Having obtained the energy of fixed μ (E_μ), this can now be substituted into the fitting equation, using the calculated coefficients a and b, to obtain the PSD at the chosen values of μ and K ($f(E_\mu, K)$, see figure 2d).

Finally, the inverse of the third adiabatic invariant, $L*$, is calculated, as step 6. $L*$ is the radial distance in the equatorial plane where an electron would reside if all external fields were removed, leaving only the internal geomagnetic field. This makes $L*$ a commonly used parameter in PSD studies. To calculate $L*$, it is required to implement a magnetic field model and the IRBEM library. Because the drift path

Initial PSD vs. L* profile

Elevated Solar Wind Pressure

Solar Wind Pressure Relaxes
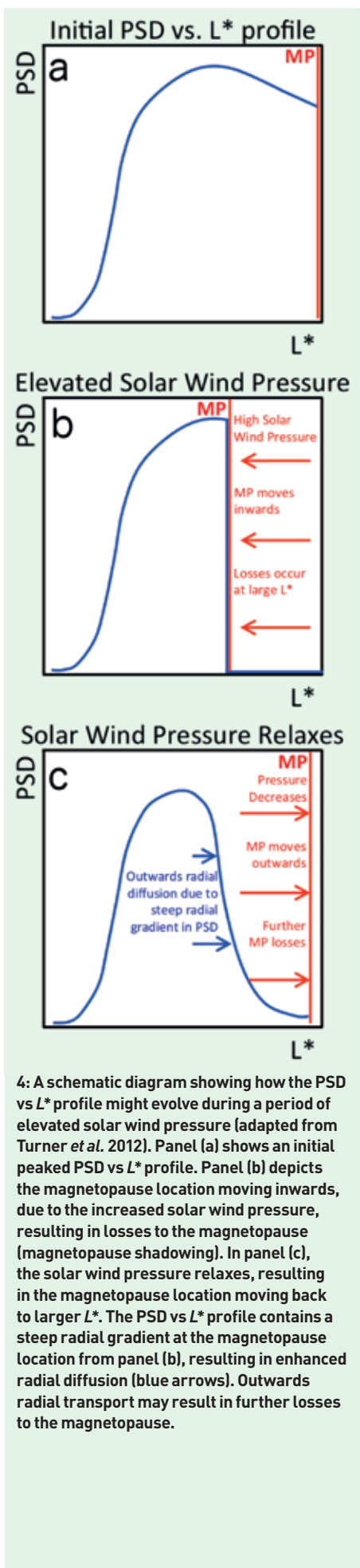
4: A schematic diagram showing how the PSD vs L^* profile might evolve during a period of elevated solar wind pressure (adapted from Turner et al. 2012). Panel (a) shows an initial peaked PSD vs L^* profile. Panel (b) depicts the magnetopause location moving inwards, due to the increased solar wind pressure, resulting in losses to the magnetopause (magnetopause shadowing). In panel (c), the solar wind pressure relaxes, resulting in the magnetopause location moving back to larger L^*. The PSD vs L^* profile contains a steep radial gradient at the magnetopause location from panel (b), resulting in enhanced radial diffusion (blue arrows). Outwards radial transport may result in further losses to the magnetopause.

of a particle depends upon its pitch angle, the pitch angle corresponding to the desired value of K, α_K, is used as an input. L^* is a direct output from the IRBEM library. This gives L^* and PSD at fixed values of the first and second adiabatic invariants, μ and K, for one time instance. This can then be repeated for each interval to provide the PSD and L^* variation at constant μ and K.

Sources and losses

Calculating the PSD vs L^* profile can assist in differentiating between internal acceleration mechanisms (local acceleration in the inner magnetosphere radiation belt region) or external acceleration (electrons transported and accelerated inwards from a seed population in the outer magnetosphere). Figure 3 is a schematic diagram showing how internal and external acceleration might look in the PSD vs L^* profile (adapted from Green and Kivelson 2004). The red lines indicate the PSD vs L^* profile before acceleration (time = t_1) with the blue line showing the effect of the acceleration event (time = t_2). It is generally accepted that external acceleration alone does not lead to negative gradients inwards of the source region because they rely on radial diffusion to transport and accelerate the electron population (see figure 3a). Therefore, a negative gradient in the PSD vs L^* profile is a strong signature of internal acceleration mechanisms that violate either the first or second adiabatic invariant (see figure 3b).

However, external acceleration mechanisms, coupled with electron losses at large L-shells, may also cause a negative gradient in the PSD vs L^* profile. These two processes may be distinguished by studying the time evolution of the PSD vs L^* profile.

Figure 4 is a schematic diagram of how specific loss mechanisms, particularly magnetopause shadowing (the loss of particles to the solar wind via the dayside magnetopause), might look in the PSD vs L^* profile (adapted from Turner et al. 2012). Figure 4a shows a PSD vs L^* profile before a solar wind pressure increase; the vertical red line indicates the magnetopause location. Figure 4b displays the PSD vs L^* profile during enhanced solar wind pressure. This increase in solar wind pressure makes the magnetopause move inwards, intersecting previously closed electron drift paths, resulting in losses. Figure 4c shows the PSD vs L^* profile once the solar wind pressure has relaxed and the magnetopause has returned to larger L^*. There is a steep radial gradient in the PSD from the magnetopause shadowing process. Radial diffusion will always act to transport particles so that PSD gradients are reduced. Such outwards transport (radial diffusion) may cause further magnetopause losses as well as an apparent "loss" at a fixed L^* due to the radial diffusion process. In order to study other loss processes (such as losses to the atmosphere through pitch-angle

scattering) it is common to couple PSD calculations with spacecraft observations in low Earth orbit (e.g. Turner et al. 2013) or with observations from the Balloon Array for RBSP Relativistic Electron Losses (BARREL) (Millan and the BARREL Team 2011, Millan et al. 2013).

Summary

Overall, PSD has been used successfully by numerous authors to investigate the processes that drive the electron radiation belt's variability (e.g. Hilmer et al. 2000, Brautigam and Albert 2000, Selesnick and Blake 2000, Green and Kivelson 2004, Chen et al. 2006, Chen et al. 2007, Turner et al. 2012, Hartley et al. 2013, Reeves et al. 2013, Schiller et al. 2014). It is the uniqueness of considering electron measurements in parallel to the geomagnetic field variations, and in a coordinate system that follows particle trajectories, that makes PSD an essential tool in solving the radiation belt riddle. ●

D P Hartley, Physics Department, Lancaster University, UK. M H Denton, Space Science Institute, Colorado, USA.

References

Baker D N et al. 2007 Geophys. Res. Lett. **34** L20110.
Brautigam D H and J M Albert 2000 J. Geophys. Res. **105** 291.
Chen Y et al. 2006 J. Geophys. Res. **111** A11S04.
Chen Y et al. 2007 Nat. Phys. **3** 614.
Friedel R H et al. 2002 J. Atmos. Sol. Terr. Phys. **64** 265.
Green J C and M G Kivelson 2004 J. Geophys. Res. **109** A03213.
Hartley D P et al. 2013 J. Geophys. Res. Space Physics **118** 6964.
Hilmer R V et al. 2000 J. Geophys. Res. **105** 23311.
Horne R B et al. 2009 Geophys. Res. Lett. **36** L19104.
IRBEM library ONERA-DESP (2004–2012), D Boscher et al. IRBEM library V4.4.0.
King J H and N E Papitashvili 2005 J. Geophys. Res. **110** A02104.
Liemohn M W and A A Chan 2007 Eos Trans. AGU **88**(42) 425.
Millan R M and the BARREL Team 2011 J. Atmos. Sol.-Terr. Phy. **73**(11–12) 1425.
Millan R M et al. 2013 Space Sci. Rev. **179** 503.
Reeves G D et al. 2013 Science **341** (6149) 991.
Schiller Q et al. 2014 Geophys. Res. Lett. **41** 7.
Schulz M and L J Lanzerotti 1974 Particle Diffusion in the Radiation Belts (Springer-Verlag, New York).
Selesnick R and J B Blake 2000 J. Geophys. Res. **105** 2607.
Shprits Y Y et al. 2012 J. Geophys. Res. **117** A01219.
Turner D L et al. 2012 Nature Physics **8** 208.
Turner D L et al. 2013 J. Geophys. Res. Space Physics **118** 2196.
Van Allen J A and L A Frank 1959 Nature **183** 430.
Van Allen J A et al. 1959 J. Geophys. Res. **64** 271.
Walt M 1994 Introduction to Geomagnetically Trapped Radiation (Cambridge University Press, Cambridge).